

# Bik subcellular localization in response to oxidative stress induced by chemotherapy, in Two different breast cancer cell lines and a Non-tumorigenic epithelial cell line

Aglaé Trejo-Vargas<sup>a,b,d</sup>, Elisa Hernández-Mercado<sup>a,b</sup>, Rosa María Ordóñez-Razo<sup>b</sup>, Roberto Lazzarini<sup>a</sup>, Diego Julio Arenas-Aranda<sup>b</sup>, María Concepción Gutiérrez-Ruiz<sup>a</sup>, Mina Königsberg<sup>a</sup> and Armando Luna-López<sup>c\*</sup>

**ABSTRACT:** Cancer chemotherapy remains one of the preferred therapeutic modalities against malignancies despite its damaging side effects. An expected outcome while utilizing chemotherapy is apoptosis induction. This is mainly regulated by a group of proteins known as the Bcl-2 family, usually found within the endoplasmic reticulum or the mitochondria. Recently, these proteins have been located in other sites and non-canonical functions have been unraveled. Bik is a pro-apoptotic protein, which becomes deregulated in cancer, and as apoptosis is associated with oxidative stress generation, our objective was to determine the subcellular localization of Bik either after a direct oxidative insult due to H<sub>2</sub>O<sub>2</sub>, or indirectly by cisplatin, an antineoplastic agent. Experiments were performed in two human transformed mammary gland cell lines MDA-MB-231 and MCF-7, and one non-tumorigenic epithelial cell line MCF-10A. Our results showed that in MCF-7, Bik is localized within the cytosol and that after oxidative stress treatment it translocates into the nucleus. However, in MDA-MB-231, Bik localizes in the nucleus and translocates to the cytosol. In MCF10A Bik did not change its cellular site after either treatment. Interestingly, MCF10A were more resistant to cisplatin than transformed cell lines. This is the first report showing that Bik is located in different cellular compartments depending on the cancer stage, and it has the ability to change its subcellular localization in response to oxidative stress. This is associated with increased sensitivity when exposed to toxic agents, thus rendering novel opportunities to study new therapeutic targets allowing the development of more active and less harmful agents. Copyright © 2015 John Wiley & Sons, Ltd.

Additional supporting information may be found in the online version of this article at the publisher's web-site.

**Keywords:** Bik; cisplatin; H<sub>2</sub>O<sub>2</sub>; oxidative stress; MCF-7; MDA-MB-23; MCF10A

## Introduction

Breast cancer is the world's second most common type of cancer and according to the WHO the most frequent in women (GLOBOCAN, 2013). Because of its diverse clinical, histological and molecular heterogeneity it is difficult to treat and predict its outcome. At present, chemotherapy is one of the mainstays as it has been successfully used as neoadjuvant and adjuvant therapy (Arowolo *et al.*, 2013; Carlson *et al.*, 2006; Jiang *et al.*, 2014). Other approaches to treat breast cancer utilize radiation or biological agents. Unfortunately, a great number of patients are resistant to these therapies resulting in disease progression, relapse and reduced survival (Jemal *et al.*, 2007; Victorino *et al.*, 2014). Therefore, it is important to develop new chemotherapeutic agents adapted to each patient's characteristics and needs.

One of the expected results while using chemotherapy is apoptosis induction. Apoptosis is a regulated cell death that can be activated by several stimuli such as oxidative stress, radiation, toxins, drugs, hormone and growth factors deprivation, it controls tissue proliferation rate by eliminating altered or damage cells. Two main mechanisms have been described to induce apoptosis; the first is the extrinsic pathway, which is activated by death

receptors such as tumor necrosis factor receptor or FAS. The second is the intrinsic pathway encompassing the mitochondrial and the endoplasmic reticulum (ER) pathways, which might be induced by different kind of stress such as DNA damage, oxidative stress, viral infections, radiations, unfolded proteins, ATP depletion, etc. The Bcl-2 proteins family is known for their participation during cellular survival regulation. These compounds have been analyzed and studied and their members have been classified as either anti- or pro-apoptotic (Chipuk *et al.*, 2010; Czabotar *et al.*,

\*Correspondence to: Armando Luna-López, Instituto Nacional de Geriatria, SSA, México, D.F. 14080, México.  
E-mail: allbioexp@yahoo.com

<sup>a</sup>Departamento de Ciencias de la Salud, DCBS, Universidad Autónoma Metropolitana Iztapalapa, México, D.F., México

<sup>b</sup>Unidad Médica en Genética Humana, Centro Médico Nacional Siglo XXI, México, D. F., Mexico

<sup>c</sup>Instituto Nacional de Geriatria, SSA, México, D.F., Mexico

<sup>d</sup>Posgrado en Biología Experimental

2014; Yang and Korsmeyer, 1996). It is also known that some Bcl-2 family members change their gene expression caused directly or indirectly by antineoplastic agents (Kontos *et al.*, 2014). Our group described that Bcl-2 also increases its expression because of mild oxidative stress (Luna-López *et al.*, 2010). Well described is the fact that some proteins in this family are able to modify their subcellular localization, which in turn completely modifies their function (Lin *et al.*, 2004). It has been suggested that Bik has a role in both, apoptosis induction and oxidative stress sensitivity (Bodet *et al.*, 2010). One interesting example is protein Bik (Chinnadurai *et al.*, 2008), which despite its pro-apoptotic role, has been found overexpressed in malignancies (García *et al.*, 2005; Lu *et al.*, 2006). The induction of Bik's expression by the transcription factor p53 or by the thyrotropic embryonic factor in response to oxidative stress has been previously reported (Ritchie *et al.*, 2009). Hence, it is important to study if Bik is also susceptible to changing its subcellular localization after oxidative stress exposure, induced by chemotherapy. Oxidative stress was generated by two different mechanisms, either directly using a known oxidant inductor such as hydrogen peroxide (H<sub>2</sub>O<sub>2</sub>) or indirectly using the chemotherapeutic agent *cis*-Diamino-Dichloro-Platin-II (*cis*platin, CP), widely used against several solid tumors (testicular, cervix, breast, ovarian, etc.) (Nardon *et al.*, 2014; Olaussen *et al.*, 2006; Shaili, 2014) and known to induce oxidative stress as part of its secondary effects (Gómez-Sierra *et al.*, 2014; Palipoch *et al.*, 2014). Three human mammary gland/breast cell lines were studied; the models were chosen due to their proliferative potential and the stage of the disease they represent. Two transformed cell lines derived from adenocarcinomas, MDA-MB-231 (ATCC HTB-26) and MCF-7 (ATCC HTB-22) were used, along with a non-tumorigenic epithelial cell line obtained from fibrocystic disease, MCF-10A (ATCC CRL 10317). It is important to remark that while MCF-7 is endocrine and chemotherapy responsive (ER+, PR+/-, HER2-), MDA-MB-231 demonstrates only an intermediate response to chemotherapy (ER-, PR-, HER2-) (Holliday and Speirs, 2011; Neve *et al.*, 2006). When grown in culture, MCF10 mammary epithelial cells present the normal structures observed in normal human breast tissue, but MCF-7 cells produce tightly cohesive structures with cell-cell adhesions, which have been associated more with cellular proliferation than with cellular metastasis (pre-metastatic stage III cancer); this is in contrast to MDA-MB-231 cells that form loosely cohesive grape-like structures consistent with a more invasive phenotype (metastatic stage IV cancer). Therefore, utilizing transformed and non-transformed cells lines are powerful experimental tools, which allow us to understand different breast cancer stages. Information obtained from these studies might translate into clinical benefits in the future (Holliday and Speirs, 2011).

Our results showed that in MCF-7, Bik is localized in the cytosol and after incubation with H<sub>2</sub>O<sub>2</sub> or CP, this protein gradually translocates into the nucleus. In MDA-MB-231 Bik localizes in the nucleus and after oxidative stress exposure it does translocate to the cytosol. In MCF10A cells, Bik did not change its cellular localization after the treatments. Interestingly, MCF10A normal cells were more resistant to CP than transformed cell lines.

Hence, we report for the first time that the anti-apoptotic protein Bik is located in different cellular compartments depending on the cancer stage, and that this protein is able to change its subcellular localization in response to oxidative stress. Apparently, this is a particular characteristic of transformed cells, which make them more susceptible to CP. More experiments are needed to determine Bik's role in such compartments, but the novel, non-apoptotic, roles revealed for the Bcl-2 family proteins, might

uncover new prospects in allowing the development of novel therapeutic agents or targets.

## Materials and methods

### Chemicals

Most chemicals and reagents were purchased from Sigma Chemical Co. (St. Louis, MO, USA). Reagents obtained from other sources are detailed throughout the text.

### Cell culture

Two breast cancer cell lines MCF-7 (ATCC no. HTB-22) and MDA-MB-231 (ATCC no. HTB-26D), and a non-tumorigenic epithelial cell line, MCF-10A (ATCC no. CRL-10317) were used in this study. MCF-7 and MDA-MB-231 cell lines were cultured in RPMI-1640 (GIBCO-BRL, Gaithersburg, MD, USA) with 10% inactivated fetal bovine serum (GIBCO-BRL), 1% non-essential amino acids, 100 U ml<sup>-1</sup> penicillin and 100 µg ml<sup>-1</sup> streptomycin (GIBCO-BRL). MCF 10A cells were grown in DMEM/F12 medium (GIBCO-BRL) and supplemented with 5% horse serum, 10 mg ml<sup>-1</sup> insulin, 100 ng ml<sup>-1</sup> cholera toxin, 20 ng ml<sup>-1</sup> epidermal growth factor and 500 ng ml<sup>-1</sup> hydrocortisone (Invitrogen, Life technologies, Carlsbad CA, USA). The medium was replaced every 3 days. Cells were trypsinized upon reaching confluence and re-plated to continue time in culture. Cells were grown at 37 °C in 60 mm diameter culture multiwell plates (Corning, Acton, MA, USA) in an atmosphere of 95% air and 5% CO<sub>2</sub>.

### Oxidative treatment and cellular viability

Cells were seeded at 1 × 10<sup>5</sup> density into 24-well plates (Corning). Cells were treated with 2, 4, 6, 8 or 16 µM CP for different times: 12, 24, 36 and 48 h. Another set of cells was treated with 200 µM H<sub>2</sub>O<sub>2</sub> for 0.5, 1, 1.5 and 2 h and cellular viability was assessed. To determine cellular viability, MCF-7, MDA-MB-231 and MCF10A treated cells were trypsinized and a 20 µl aliquot was stained with an equal volume of a 0.4% trypan blue physiological solution (trypan blue exclusion). The number of living cells in 10 µl of this suspension was scored using five fields of a hemocytometer under a phase contrast optical microscope as described elsewhere (López-Diazguerrero *et al.*, 2006).

### Immunofluorescence assay

MCF-7, MDA-MB-231 and MCF10A treated cells were washed with phosphate-buffered saline (PBS) and fixed with 4% paraformaldehyde for 30 min; immediately thereafter, cells were incubated in blocking buffer (2% bovine serum albumin, 0.2% non-fat milk, 0.4% Triton X100 in PBS) for 1 h at room temperature. Immunofluorescence was performed as describe elsewhere (Alarcón-Aguilar *et al.*, 2014). Briefly, cells were washed and incubated for one more hour with the primary antibody anti-Bik (ab52182; Abcam, Cambridge, MA, USA). Cells were washed three times with PBS-Tween 0.2% and were incubated with the secondary antibody (ALEXA 488 dilution 1: 200). After four more washes, cells were further incubated with DAPI (10 µg ml<sup>-1</sup>) for 10 min to stain the DNA and mark the nucleus. Cells were washed twice again and mounted with fluorescent mounting medium (Dako Cytomation, Glostrup, Denmark). Singles plane images were obtained with a confocal microscope LSM-780-NLO-Zeiss imaging at 40× with

the Diodo Laser 405 nm for DAPI and Ar/ML 458/488/514 nm for ALEXA FLUOR-488. Nuclear and cytosolic localization analysis was specially performed using the ZEN2010 version 6.0 (Carl Zeiss, Oberkochen, Germany).

### Statistical analysis

Data are reported as the means  $\pm$  SD for at least three independent experiments performed by triplicate. The ANOVA test followed by the Tukey-Kramer Test, were used to compare data. A 0.05 level of probability was used as a minimum criterion of significance.

## Results

### Cisplatin effect on cellular viability in breast cancer cell lines

To determine the concentration of CP that would be used to evaluate Bik subcellular localization in MCF-7, MDA-MB-231 and MCF10-A, cellular viability was evaluated in all cell lines after CP treatment at different concentrations (0–16  $\mu$ M) and time points (12, 24, 36, 48 h). Eight and 16  $\mu$ M CP reduced more than 50% viability during the first 12 h and killed 100% of all three line cells at 48 h; therefore, those results are not shown in the figures. As observed in Fig. 1(A), MCF-7 cells decreased 10% of their viability when treated with 2  $\mu$ M CP for 12 h and achieved their lower viability (30% decrease) at 48 h. While with 4  $\mu$ M CP, viability diminished 37% after 12 h treatment with a maximum of 77% reduction after 48 h. With 6  $\mu$ M CP during the same determined time points, viability decreased 35% at 12 and 48% at 24 h, finding a greater decline (more than 70%) during the following hours. The viability changes during all the treatments studied

were statistically different against the control ( $P < 0.0001$ ) with the exception of 2  $\mu$ M CP at 12 h.

The effect of CP treatment on MDA-MB-231 viability is shown in Fig. 1(B). No effects were observed during the first 24 h of the 2  $\mu$ M CP treatment, but viability drastically decreased, 66%, at 36 h and 74% at 48 h. With 4  $\mu$ M CP at the evaluated time points, cellular viability diminished 13%, 21%, 78% and 85% respectively; and with 6  $\mu$ M CP the same behavior was observed, a low effect during the first 24 h but a drastic decrease at 36 h (87%) and at 48 h (93%). CP also inhibited viability in the cell line MDA-MB-231 in dose- and time-dependent manner. In MCF10A, cellular viability (Fig. 1(C)) only diminished 20% during the first 24 h for 2 and 4  $\mu$ M CP and 25% at 6  $\mu$ M CP. The higher decreases were observed until 36 h (50%) and 48 h (75%). Taking into consideration all the aforementioned experiments, 6  $\mu$ M for 24 h were the chosen conditions used in the next experiments, as at those conditions approximately 50% viability was still maintained in all cell lines and significant differences were observed among them (Fig. 1(D)).

### H<sub>2</sub>O<sub>2</sub> effect on cellular viability in breast cancer cell lines

Previous data from our lab and others (Burdon, 1995; Luna-López *et al.*, 2010; Pickering *et al.*, 2012; Wiese *et al.*, 1995) have shown that 200  $\mu$ M H<sub>2</sub>O<sub>2</sub> is an effective dose to induce acute cellular damage at short times without killing the cells. However, to determine the best induction time, all three cell lines were treated with 200  $\mu$ M H<sub>2</sub>O<sub>2</sub> at diverse short times, 0.5, 1, 1.5 and 2 h. MCF-7 viability after 30 min treatment with H<sub>2</sub>O<sub>2</sub> diminished approximately 10%; 23% after 1 h and 55% at 2 h (Fig. 2A). All the data were significantly different from the control ( $P < 0.005$ ). H<sub>2</sub>O<sub>2</sub> treatment on the cell line MDA-MB-231 showed the same behavior (Fig. 2B).

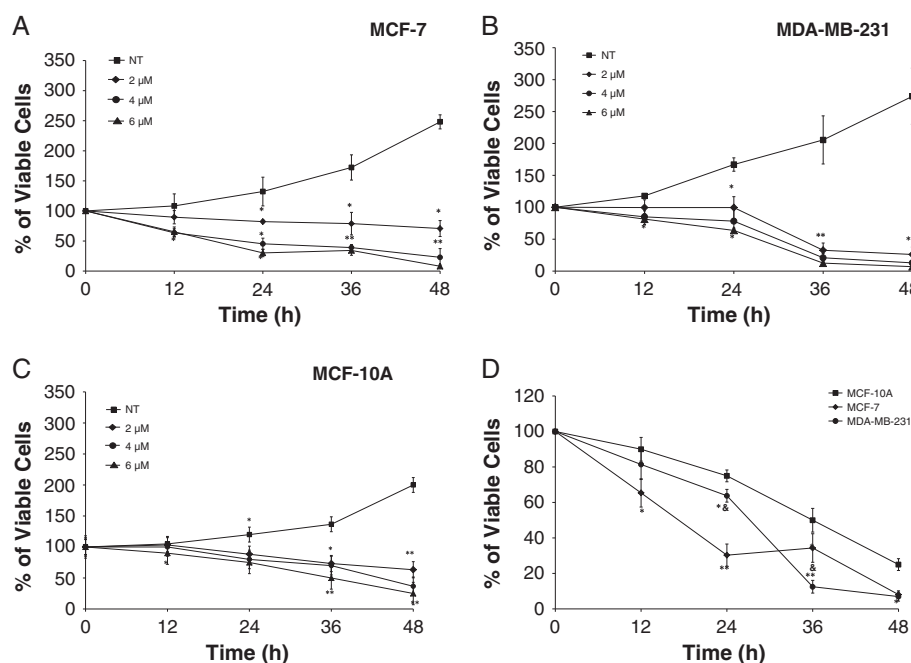


**Figure 1.** CP effect on cellular viability. CP effect on cellular viability was assessed in three different breast cancer cell lines. (A) MCF-7, (B) MDA-MB-231 and (C) MCF10A cells were treated with different CP concentrations 2, 4, 6  $\mu$ M for 12, 24, 36 and 48 h, and their viability was determined as describe in material and methods. Statistical significance with respect to untreated cells \* $P < 0.05$ , \*\* $P < 0.01$  was considered. (D) Comparison among the cell lines during 6  $\mu$ M CP treatment. Statistical significance with respect to MCF10A cells \* $P < 0.05$ , \*\* $P < 0.01$  and & $P < 0.05$  with respect MCF-7 cells. Each point represents the mean  $\pm$  SD of nine determinations performed in three independent experiments. CP, cisplatin.

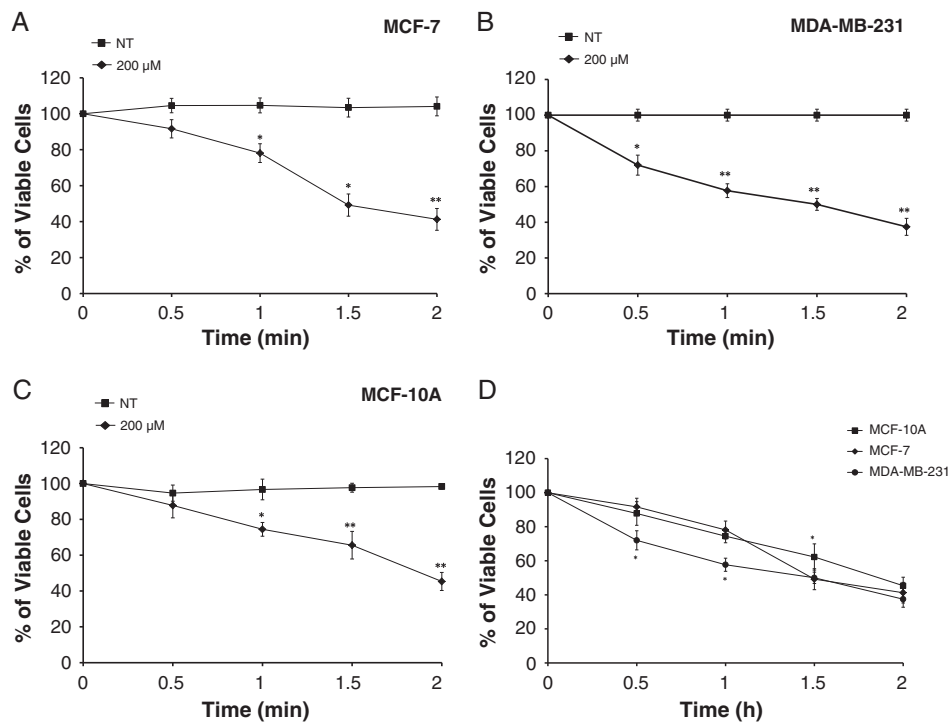


**Figure 2.**  $\text{H}_2\text{O}_2$  effect on cellular viability.  $\text{H}_2\text{O}_2$  effect on cellular viability was assessed in three different breast cancer cell lines. (A) MCF-7, (B) MDA-MB-231 and (C) MCF10A cells were treated with  $200 \mu\text{M}$   $\text{H}_2\text{O}_2$  for 0.5, 1, 1.5 and 2 h, and their viability was determined as described in Materials and methods. Statistical significance with respect to untreated cells  $*P < 0.05$ ,  $**P < 0.01$  was considered. (D) Comparison among the cell lines during  $200 \mu\text{M}$   $\text{H}_2\text{O}_2$  treatment. Statistical significance with respect to MCF10A cells  $*P < 0.05$ ,  $**P < 0.01$ . Each point represents the mean  $\pm$  SD of nine determinations performed in three independent experiments.

There was a 28% viability decrease after 30 min treatment, while after 1 h viability diminished 42% and 58% at 2 h. All the data were significantly different from the control ( $P < 0.005$ ); therefore, 2 h was also chosen for MDA-MB-231. Interestingly, MCF10A that were more resistant to CP, showed a higher susceptibility to  $\text{H}_2\text{O}_2$ , particularly at short time periods. Viability decreased 25% after 30 min treatment, 42% after 1 h and 60% at 2 h (Fig. 2C). Two hours was the time chosen for the next experiments because nearly 50% of cellular viability was preserved.

### Bik subcellular localization after cisplatin treatment

Bik subcellular localization after  $6 \mu\text{M}$  CP treatment was evaluated by immunofluorescence in MCF-7 cells from 6 to 36 h. Fig. 3(A) shows that Bik is localized in the cytoplasm in untreated cells and that from 6 to 12 h its level increases. After 24 h and until 36 h, Bik changes its location and is mainly observed in the nucleus. This was corroborated by Bik colocalization with the fluorescent marker DAPI, which adheres to enriched adenine and thymine regions in DNA; thus, suggesting that Bik translocates into the nucleus in response to CP treatment in MCF-7 cells. Two videos are presented in the Supporting information: Video 1 shows that Bik is prominently outside the nucleus in untreated MCF-7 cells and Video 2 shows that after 24 h CP treatment Bik is found in the nucleus.

MDA-MB-231 immunofluorescences revealed a different scenario. Figure 3(B) shows that in this case, Bik localizes in the nucleus in untreated cells (Video 3, Supporting information), but after the 6 h treatment it leaves the nucleus. At 12 h, an increase in the fluorescent signal is observed, both in nucleus and in the cytosol,

suggesting an augmented protein expression and a change in localization. At 24 h, the Bik signal in the cytosol fades, but it is still maintained in the nucleus, and at 36 h, it almost disappears in both sites. Interestingly, in MCF10A Bik's signal increased with time, particularly at 24 and 36 h (Fig. 3C) (Video 4, Supporting information), implying again an increase in protein expression, but it always remained in the cytosol and did not translocate into the nucleus.

Figure 3(D,E) shows the Z-stack analysis performed using the ZEN 2010 program version 6.0 (Carl Zeiss). Ortho and 3D images were obtained to determine and quantify Bik nuclear and cytosolic localization and the image reconstruction generated a video clearly showing Bik behavior. These results confirm that in MDA-MB, Bik had a dynamic behavior, it left the nucleus soon after CP treatment (6 h), but it re-entered repeatedly during subsequent hours. While in MCF7, Bik slowly translocated into the nucleus achieving its maximal point at 24 h. Remarkably, Bik was not detected in the MCF10A nucleus at any time during CP treatment.

### Bik subcellular localization after $\text{H}_2\text{O}_2$ treatment

Bik subcellular localization after  $\text{H}_2\text{O}_2$  displayed a similar behavior to that observed with CP. In MCF-7 non-treated cells and after the shorter incubation times, 0.5 h and 1 h, the signal appears mostly in the cytosol (Fig. 4A); however, at 24 h Bik colocalizes with DAPI in the nucleus, in agreement with the previous results where Bik translocates into the nucleus after an oxidative insult. In the MDA-MB-231 cell line (Fig. 4B), Bik is seen again in the untreated cell nucleus, but after 2 h of  $\text{H}_2\text{O}_2$

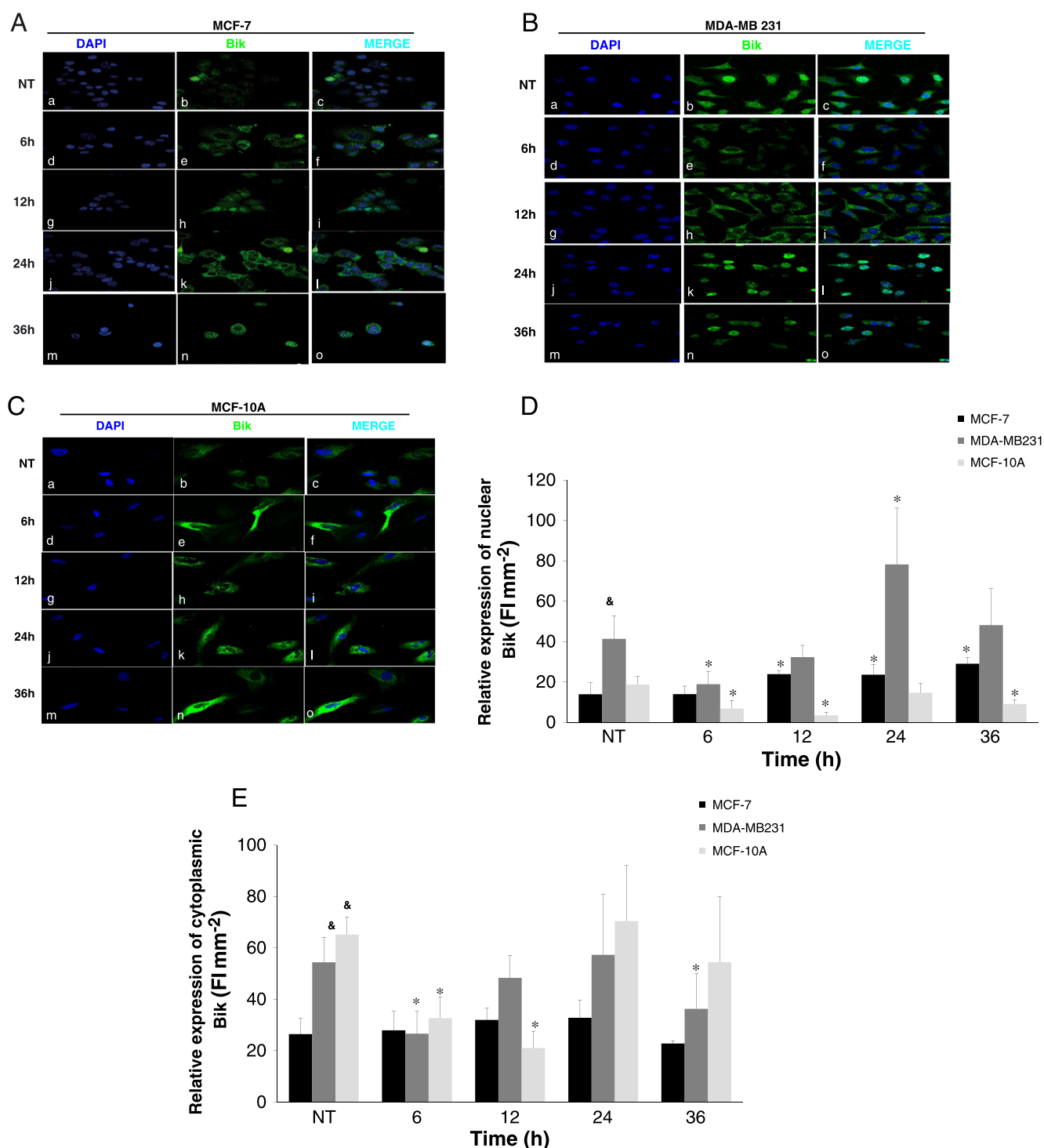


**Figure 3.** Bik subcellular localization during cisplatin treatment. Confocal microscopic images of (A) MCF-7, (B) MDA-MB-231 and (C) MCF10A cells treated with 6  $\mu\text{M}$  CP as described in Materials and methods. Immunofluorescence was evaluated at 6, 12, 24 and 36 h. In a, d, g, j and m, Bik immunostaining (green); in b, e, h, k and n, DAPI staining (blue); in c, f, i, l and o, merge. Single plane images were obtained with a confocal microscope LSM-780-NLO-Zeiss imaging at 40 $\times$  with the Diodo Laser 405 nm for DAPI and Ar/ML 458/488/514 nm for ALEXA FLUOR-488. Nuclear and cytosolic localization analysis was particularly performed using the ZEN2010 version 6.0 (Carl Zeiss). (D) Analysis of Bik in the nucleus. (E) Analysis of Bik in the cytosol. The co-immunolocalization of Bik (green) with the DNA marker (DAPI) was done throughout the complete timeline course during CP treatment. Colocalization was determined using Zen 2010 program version 6.0. Each point represents the mean  $\pm$  SD of three determinations performed in independent experiments. MCF-7 (black bars), MDA-MB-231 (grey bars) and MCF10A (white bars). Statistical significance with respect to each untreated cell type control (NT): \* $P < 0.05$ , \*\* $P < 0.01$ , \*\*\* $P < 0.001$  were considered. &  $P < 0.05$  with respect to MCF-7.

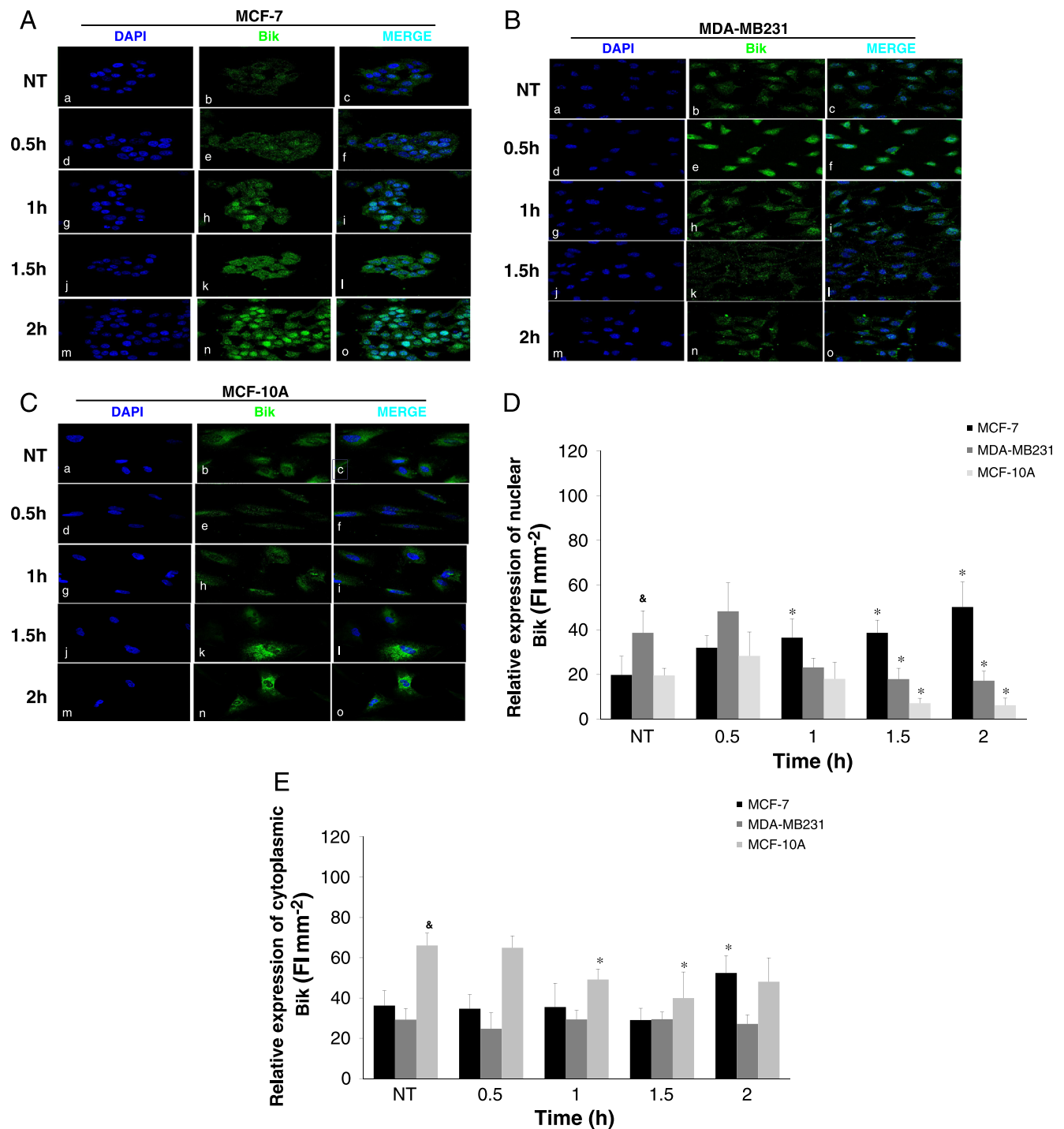


**Figure 4.** Bik subcellular localization during  $H_2O_2$  treatment. Confocal microscopic images of (A) MCF-7, (B) MDA-MB-231 and (C) MCF10A cells treated with  $200 \mu M H_2O_2$  as described in Materials and methods. Immunofluorescence was evaluated at 6, 12, 24 and 36 h. In a, d, g, j and m, Bik immunostaining (green); in b, e, h, k and n, DAPI staining (blue); in c, f, i, l and o, merge. Single plane images were obtained with a confocal microscope LSM-780-NLO-Zeiss imaging at  $40\times$  with the Diodo Laser 405 nm for DAPI and Ar/ML 458/488/514 nm for ALEXA FLUOR-488. Nuclear and cytosolic localization analysis was particularly performed using the ZEN2010 version 6.0 (Carl Zeiss). (D) Analysis of Bik in the nucleus. (E) Analysis of Bik in the cytosol. The co-immunolocalization of Bik (green) with the DNA marker (DAPI) was done throughout the complete timeline course during  $H_2O_2$  treatment. Co-localization was determined using Zen 2010 program version 6.0. Each point represents the mean  $\pm$  SD of three determinations performed during independent experiments. MCF-7 (black bars), MDA-MB-231 (gray bars) and MCF10A (white bars). Statistical significance with respect to each untreated cell type control (NT): \* $P < 0.05$ , \*\* $P < 0.01$ , \*\*\* $P < 0.001$  were considered. &  $P < 0.05$  with respect to MCF-7.

treatment the fluorescent signal increased in the cytosol, while the signal decreased in the nucleus, suggesting Bik nuclear withdrawal, and ratifying the same effect observed after MDA-

MB-231 CP treatment. In the MCF10A cell line the Bik fluorescent signal gradually increased after  $H_2O_2$  treatment, but the signal was always observed in the cytosol (Fig. 4C), indicating

that Bik was not being translocated into the nucleus. Fig. 4(D,E) show Bik nuclear and cytosolic localization performed using the ortho and 3D images with the Z-stack analysis (Supporting information). The figure shows that in the MDA-MB cell, Bik that was originally in the nucleus slowly relocated to the cytosol. In MCF7, the maximal Bik accumulation in the nucleus was observed at 24 h, while Bik was not detected in the MCF10A nucleus at any time during H<sub>2</sub>O<sub>2</sub> treatment. It is remarkable to notice that there is a significant difference between Bik nuclear signal intensity in MDA-MB cells in comparison to MCF-7 cells, thus confirming that this antiapoptotic protein has a different subcellular localization in both cell lines before any treatment; this might be related to the cancer stage and the properties inherent to each cell line.

## Discussion

The role of Bcl-2 family proteins has been re-evaluated, as some of them are altered in cancer (Kontos *et al.*, 2014; Safaeian *et al.*, 2014). In particular, the pro-apoptotic protein Bik, who has been found overexpressed in malignancies (García *et al.*, 2005; Lu *et al.*, 2006). Most chemotherapeutic drugs are known for their capacity to generate reactive oxygen species and induce oxidative stress. This could favor some cancer subpopulations survival and at the same time generating chemotoxicity in non-malignant cells (Mahalingaiah and Singh, 2014; Victorino *et al.*, 2014). Hence, it is important to explore if pro-apoptotic proteins are able to change their subcellular localization in function of redox state changes, which might explain these contradictory effects and might allow the development of a new generation of chemotherapeutic agents with less side effects. Based on previous evidence, we wanted to determine Bik subcellular localization in two breast cancer cell lines with different characteristics, MCF-7 and MDA-MB-231, as well as a normal breast epithelial cell line, MCF10A, after treating them with a chemotoxic and an oxidant agent, which indirectly and directly induce oxidative stress. CP is one of the stronger antitumor agents used against solid tumors (Armstrong *et al.*, 2006; Olaussen *et al.*, 2006; Worden *et al.*, 2006). Its toxic effect is mediated by its interaction with DNA forming covalent adducts, which impede DNA strand separation and therefore, replication and transcription, activating mitochondrial apoptotic pathway (García *et al.*, 2007), along with mitochondrial reactive oxygen species generation (Cardinaal *et al.*, 2004). On the other hand, the oxidant agent used was H<sub>2</sub>O<sub>2</sub>, because it is one of the oxidative stress inductors, which when used at adequate doses is able to trigger apoptotic cell death (Bauer 2014; Katsube *et al.*, 2014). The CP and H<sub>2</sub>O<sub>2</sub> concentrations used here were determined based on previous reports by our group and others (Luna-López *et al.*, 2010; Mahalingaiah and Singh, 2014; Sarangi *et al.*, 2013) and were adjusted to the particular conditions of the cell lines used.

A new finding was Bik localization in MDA-MB-231 nucleus because this is an unusual and non-reported localization. Until now, Bik has been mainly detected in the ER and in the mitochondria (Germain *et al.*, 2002; Szegezdi *et al.*, 2009). Instead and concurring with previous reports, Bik was found in the cytoplasm of MCF-7 cells. After treating the cells, Bik changed its position on both of them in an opposite manner; it translocates into the nucleus in MCF-7 cells and it went out of it in MDA-MB-231 (Figs. 3 and 4). Even when we did not evaluate the

function that these changes in localization might mean, this is a relevant result because of its implications. As the subcellular distribution was different in the two cell lines, representing distinctive stages of the disease. It is remarkable to notice that there is a significant difference between Bik nuclear signal intensity in MDA-MB cells in comparison to MCF-7 cells, thus confirming that this anti-apoptotic protein has a different subcellular localization in both cell lines probably related to the cancer stage and the properties inherent to each cell line.

In regards to the normal cell line, Bik did not change its subcellular localization. Interestingly, MCF-10A cells showed a higher resistance to CP treatment than transformed cells, which suggests that Bik translocation might be related to a particular function during tumorigenesis, perhaps related to promoting increased proliferation or metastasis, but not related to cell survival. Moreover, to gain that "tumorigenic" feature, transformed cells might probably have to forego several survival and/or protecting mechanisms.

Still, it was not totally unexpected to find Bik in a different cellular compartment in the transformed cell lines, as lately it has been described that several members of the Bcl-2 family are in unusual positions, performing different functions to the canonically reported (Danial *et al.*, 2008; Martinou and Youle, 2011). Despite the fact that these proteins are known for their participation in apoptosis, there is strong evidence that suggests that BH3-only proteins are involved in other vital functions beyond their role in cell death, including functions in nutrient metabolism (Hetz and Glimcher, 2008). For example, it was recently reported that Bax, constitutively targeted to mitochondria, is constantly translocated back to the cytosol in non-apoptotic cells and it only stays and accumulates there when cell death is induced (Schellenberg *et al.*, 2013). The best example is Bad, which encompasses distinctive roles; it has been involved in cell cycle progression when it dimerizes with Bcl-xL, avoiding cell arrest in G<sub>0</sub>/G<sub>1</sub> phase (Chattopadhyay *et al.*, 2001). The overexpression of Bad was not only associated with cell cycle progression, but with interleukin-2 production after T-cell activation because of AKT regulation (Mok *et al.*, 1999).

Danial and co-workers found another physiological role for Bad during insulin secretion by  $\beta$ -pancreatic cells. This new role depends on BH3 phosphorylation in Ser 155, which inactivates its pro-apoptotic function and is required for its activation during glucose-stimulated insulin secretion (Danial *et al.*, 2008). In brain, Bad has been found in several anatomic locations, including those involved in nutrients and glucose regulation (Bu and Lephart, 2005).

Another example is the pro-apoptotic protein Bid, who has recently been described as a critical mediator during inflammation and innate immunity (Garrett *et al.*, 2010; Takeuchi and Akira, 2010). Bid has also been implicated in lipid transfer between mitochondrial membrane and other cellular membranes, granting this protein a role in mitochondrial phospholipid transport and recycling (Esposti *et al.*, 2001). Bid has dual roles with respect to the stress response, it is involved in the DNA damage response and its phosphorylation may negatively regulate its pro-apoptotic function (Song *et al.*, 2010).

All the above suggests that Bik could also be involved in processes that do not necessarily imply its participation in apoptosis. There are some reports where Bik has been proposed to interact with transcription factors, such as ERK 1/2, independently of its BH3 domain (Mebratu *et al.*, 2008). Bik direct interaction impedes transcription factors to translocate into the nucleus. Interestingly,

when apoptosis is stimulated by an oxidative inductor in cell lines that express p53 in a wild-type manner, such as MCF-7, p53 is known to translocate into the nucleus. This nuclear translocation is not observed in cell lines with mutated p53 or knockouts such as MDA-MB-231 and SKOV3 (Truong *et al.*, 2014; Xuan *et al.*, 2014). Therefore, Bik might be participating or favoring p53 nuclear translocation during the oxidative stress response in MCF-7 cells. Another study associates Bik with ER calcium levels and autophagy regulation (Leber and Andrews 2010; Maiuri *et al.*, 2010). Bik is known to form heterodimers with anti-apoptotic family members such as Bcl-2 and Bcl-xL during apoptosis (Chinnadurai *et al.*, 2008); therefore, Bik is able to displace Bcl-2 from the complex it forms with nutrient-deprivation autophagy factor-1. Nutrient-deprivation autophagy factor-1 physically associates with the ER inositol 1,4,5-triphosphate  $Ca^{2+}$  leak channel and is required for Bcl-2-dependent channel regulation (Chang *et al.*, 2012); Bik displacement allows  $Ca^{2+}$  release from the ER, thus promoting autophagy (Maiuri *et al.*, 2010; Szegezdi *et al.*, 2009).

Nevertheless, some important facts remain to be elucidated, the most important challenge is to try to understand what is Bik's role in the nucleus, and if that function implies changes in gene transcription. Another question is to determine which protein or chaperone translocates Bik and why the different cell lines that represent dissimilar cancer stages present different Bik locations. However, the finding that Bik did not change its subcellular localization in MCF-10A cells, and that those cells were more resistant to CP treatment opens a new avenue to study new therapeutic targets. Finally, the answer to these questions will certainly lead us to a better understanding of the role of Bcl-2 proteins in cancer and will allow us to develop better therapies with less secondary and harmful effects.

### Acknowledgments

The authors would like to thank the CBS-UAMI Confocal Core for the acquisition of confocal images and analysis. This work was supported by CONACyT's grant CB 2012-1-178349, in addition to the "Red Temática de Investigación en Salud y Desarrollo Social" from CONACyT and INGER DI-PI004/2012. A.V.-T. is a CONACyT and IMSS scholarship holder.

### Conflict of interest

The authors did not report any conflict of interest.

### References

Alarcón-Aguilar A, Luna-López A, Ventura-Gallegos JL, Lazzarini R, Galván-Arzate S, González-Puertos VY, Morán J, Santamaría A, Königsberg M. 2014. Primary cultured astrocytes from old rats are capable to activate the Nrf2 response against MPP+ toxicity after tBHQ pre-treatment. *Neurobiol. Aging* **35**: 1901–1912.

Armstrong KD, Bundy B, Wenzel L, Huang HQ, Baergen R, Lele S, Copeland LJ, Walker JL, Burger RA. 2006. Intraperitoneal Cisplatin and Paclitaxel in ovarian cancer. *N. Engl. J. Med.* **354**: 34–43.

Arowolo OA, Njiaju UO, OgunDIRAN TO, Abidoye O, Lawal OO, Obajimi M, Adetiloye AV, Im HK, Akinkuolie AA, Oluwasola A, Adelusola K, Kayode AA, Agbakwuru AE, Oduntan H, Babalola CP, Fleming G, Olopade OC, Falusi AG, Durosini MA, Olopade OI. 2013. Neo-adjuvant capecitabine chemotherapy in women with newly diagnosed locally advanced breast cancer in a resource-poor setting (Nigeria): efficacy and safety in a phase II feasibility study. *Breast J.* **19**: 470–477.

Bauer G. 2014. Targeting extracellular ROS signaling of tumor cells. *Anticancer Res* **34**: 1467–1482.

Bodet L, Ménoret E, Descamps G, Pellat-Deceunynck C, Bataille R, Le Guillou S, Moreau P, Amiot M, Gomez-Bougie P. 2010. BH3-only protein Bik is

involved in both apoptosis induction and sensitivity to oxidative stress in multiple myeloma. *Br. J. Cancer* **103**: 1808–1814.

Bu L, Lephart ED. 2005. Soy isoflavones modulate the expression of BAD and neuron-specific beta III tubulin in male rat brain. *Neurosci. Lett.* **385**: 153–157.

Burdon R. 1995. Superoxide and hydrogen peroxide in relation to mammalian cell proliferation. *Free Radic. Biol. Med.* **18**: 775–794.

Cardinaal RM, De Groot JC, Huizing EH, Smoorenburg GF, Veldman JE. 2004. Ultrastructural changes in the albino guinea pig cochlea at different survival times following cessation of 8-day cisplatin administration. *Acta Otolaryngol.* **124**: 144–154.

Carlson RW, Carlson MD, Brown E, Burstein HJ, Gradishar WJ, Hudis CA, Loprinzi C, Mamounas EP, Perez EA, Pritchard K, Ravdin P, Recht A, Somlo G, Theriault RL, Winer EP, Wolff AC; National Comprehensive Cancer Network. 2006. NCCN Task Force Report: Adjuvant Therapy for Breast Cancer Task Force. *J. Natl. Compr. Cancer Netw.* **4**: S1–S26.

Chang NC, Nguyen M, Bourdon J, Risse PA, Martin J, Danialou G, Rizzuto R, Petrof BJ, Shore GC. 2012. Bcl-2-associated autophagy regulator Naf-1 required for maintenance of skeletal muscle. *Hum. Mol. Genet.* **21**: 2277–2287.

Chattopadhyay A, Chiang CW, Yang E. 2001. BAD/BCL-X(L) heterodimerization leads to bypass of G0/G1 arrest. *Oncogene* **20**: 4507–4518.

Chinnadurai G, Vijayalingam S, Rashmi R. 2008. BIK, the founding member of the BH3-only family proteins: mechanisms of cell death and role in cancer and pathogenic processes. *Oncogene* **27**: S20–S29.

Chipuk JE, Moldoveanu T, Llambi F, Parsons MJ, Green DR. 2010. The BCL-2 family reunion. *Mol. Cell* **37**: 299–310.

Czabotar PE, Lessene G, Strasser A, Adams JM. 2014. Control of apoptosis by the BCL-2 protein family: implications for physiology and therapy. *Nat. Rev. Mol. Cell Biol.* **15**: 49–63.

Daniel NN, Walensky LD, Zhang CY, Choi CS, Fisher JK, Molina AJ, Datta SR, Pitter KL, Bird GH, Wikstrom JD, Deeney JT, Robertson K, Morash J, Kulkarni A, Neschen S, Kim S, Greenberg ME, Corkey BE, Shirihai OS, Shulman GI, Lowell BB, Korsmeyer SJ. 2008. Dual role of proapoptotic BAD in insulin secretion and beta cell survival. *Nat. Med.* **14**: 144–153.

Esposti MD, Erler JT, Hickman JA, Dive C. 2001. Bid, a widely expressed proapoptotic protein of the Bcl-2 family, displays lipid transfer activity. *Mol. Cell. Biol.* **21**: 7268–7276.

García BJR, Nevado J, Ramírez CR, Sanz R, González GJA, Sánchez RC, Cantos B, España P, Verdaguer JM, Trinidad CA. 2007. The anticancer drug cisplatin induces an intrinsic apoptotic pathway inside the inner ear. *Br. J. Pharmacol.* **152**: 1012–1020.

García N, Salamanca F, Astudillo-de la Vega H, Curiel-Quesada E, Alvarado I, Peñaloza R, Arenas D. 2005. A molecular analysis by gene expression profiling reveals *Bik/NBK* overexpression in sporadic breast tumor samples of Mexican females. *BMC Cancer* **1**: 93.

Garrett WS, Gordon JI, Glimcher LH. 2010. Homeostasis and inflammation in the intestine. *Cell* **140**: 859–870.

Germain M, Mathai JP, Shore GC. 2002. BH-3-only BIK functions at the endoplasmic reticulum to stimulate cytochrome c release from mitochondria. *J. Biol. Chem.* **277**: 18053–18060.

GLOBOCAN. 2013. Cancer Incidence and Mortality Worldwide. International Agency for Research on Cancer. 2013. Available from: <http://globocan.iarc.fr> (accessed on July 15, 2014).

Gómez-Sierra T, Molina-Jijón E, Tapia E, Hernández-Pando R, García-Niño WR, Maldonado PD, Reyes JL, Barrera-Oviedo D, Torres I, Pedraza-Chaverri J. 2014. S-allylcysteine prevents cisplatin-induced nephrotoxicity and oxidative stress. *J. Pharm. Pharmacol.* **14**: 111.

Hetz C, Glimcher L. 2008. The daily job of night killers: alternative roles of the BCL-2 family in organelle physiology. *Trends Cell Biol.* **18**: 38–44.

Holliday DL, Speirs V. 2011. Choosing the right cell line for breast cancer research. *Breast Cancer Res.* **13**: 215–222.

Jemal A, Siegel R, Ward E, Murray T, Xu J, Thun MJ. 2007. Cancer statistics. *CA Cancer J. Clin.* **57**: 43–66.

Jiang YZ, Yu KD, Bao J, Peng WT, Shao ZM. 2014. Favorable prognostic impact in loss of TP53 and PIK3CA mutations after neoadjuvant chemotherapy in breast cancer. *Cancer Res.* **74**: 3399–3407.

Katsube T, Mori M, Tsuji H, Shiomi T, Wang B, Liu Q, Neno M, Onoda M. 2014. Most hydrogen peroxide-induced histone H2AX phosphorylation is mediated by ATR and is not dependent on DNA double-strand breaks. *J. Biochem.* **156**: 85–95.

Kontos CK, Christodoulou MI, Scorilas A. 2014. Apoptosis-related BCL2-family members: Key players in chemotherapy. *Anticancer Agents Med Chem.* **14**: 353–374.

- Leber B, Andrews DW. 2010. Closing in on the link between apoptosis and autophagy. *F1000 Biol. Rep.* **2**: 88.
- Lin B, Kolluri SK, Lin F, Liu W, Han YH, Cao X, Dawson MI, Reed JC, Zhang XK. 2004. Conversion of Bcl-2 from protector to killer by interaction with nuclear orphan receptor Nur77/TR3. *Cell* **116**: 527–540.
- López-Díazguerrero NE, López-Araiza H, Conde-Perezprina JC, Bucio L, Cárdenas-Aguayo MC, Ventura JL, Covarrubias L, Gutiérrez-Ruiz MC, Zentella A, Königsberg M. 2006. Bcl-2 protects against oxidative stress while inducing premature senescence. *Free Radic. Biol. Med.* **40**: 1161–1169.
- Lu Y, Lemon W, Liu PY, Yi Y, Morrison C, Yang P, Sun Z, Szoke J, Gerald WL, Watson M, Govindan R, You M. 2006. A gene expression signature predicts survival of patients with stage I non-small cell lung cancer. *PLoS Med.* **3**: e467.
- Luna-López A, Triana-Martínez F, López-Díaz Guerrero NE, Ventura-Gallegos JL, Gutiérrez-Ruiz MC, Damián-Matsumura P, Zentella A, Gómez-Quiroz LE, Königsberg M. 2010. Bcl-2 sustains hormetic response by inducing Nrf-2 nuclear translocation in L929 mouse fibroblasts. *Free Radic. Biol. Med.* **49**: 1192–1204.
- Mahalingaiah PK, Singh KP. 2014. Chronic oxidative stress increases growth and tumorigenic potential of MCF-7 breast cancer cells. *PLoS One* **9**: e93799.
- Maiuri MC, Ciriolo A, Kroemer G. 2010. Crosstalk between apoptosis and autophagy within the Beclin 1 interactome. *EMBO J.* **29**: 515–516.
- Martinou JC, Youle RJ. 2011. Mitochondria in apoptosis: Bcl-2 family members and mitochondrial dynamics. *Dev. Cell* **21**: 92–101.
- Mebratu YA, Dickey BF, Evans C, Tesfaigzi Y. 2008. The BH3-only protein Bik/Bik/Nbk inhibits nuclear translocation of activated ERK1/2 to mediate IFN gamma-induced cell death. *J. Cell Biol.* **183**: 429–439.
- Mok CL, Gil-Gómez G, Williams O, Coles M, Taga S, Tolaini M, Norton T, Kioussis D, Brady HJ. 1999. Bad can act as a key regulator of T cell apoptosis and T cell development. *J. Exp. Med.* **189**: 575–586.
- Nardon C, Boscutti G, Fregona D. 2014. Beyond platinum: gold complexes as anticancer agents. *Anticancer Res* **34**: 487–492.
- Neve RM, Chin K, Fridlyand J, Yeh J, Baehner FL, Fevr T, Clark L, Bayani N, Coppe JP, Tong F, Speed T, Spellman PT, DeVries S, Lapuk A, Wang NJ, Kuo WL, Stilwell JL, Pinkel D, Albertson DG, Waldman FM, McCormick F, Dickson RB, Johnson MD, Lippman M, Ethier S, Gazdar A, Gray JW. 2006. A collection of breast cancer cell lines for the study of functionally distinct cancer subtypes. *Cancer Cell* **10**: 515–527.
- Olaussen KA, Dunant A, Fouret P, Brambilla E, André F, Haddad V, Taranchon E, Filipits M, Pirker R, Popper HH, Stahel R, Sabatier L, Pignon JP, Tursz T, Le Chevalier T, Soria JC. 2006. DNA repair by ERCC1 in non-small-cell lung cancer and cisplatin-based adjuvant chemotherapy. *N. Engl. J. Med.* **355**: 983–991.
- Palipoch S, Punsawad C, Koomhin P, Suwannalert P. 2014. Hepatoprotective effect of curcumin and alpha-tocopherol against cisplatin-induced oxidative stress. *BMC Comp. Altern. Med.* **14**: 111.
- Pickering AM, Linder RA, Zhang H, Forman HJ, Davies KJ. 2012. Nrf2-dependent induction of proteasome and Pa28 alpha-beta regulator are required for adaptation to oxidative stress. *J. Biol. Chem.* **287**: 10021–10031.
- Ritchie A, Gutiérrez O, Fernández JL. 2009. PAR bZIP-bik is a novel transcriptional pathway that mediates oxidative stress-induced apoptosis in fibroblasts. *Cell Death Differ.* **16**: 838–846.
- Safaeian L, Abed A, Vaseghi G. 2014. The role of Bcl-2 family proteins in pulmonary fibrosis. *Eur. J. Pharmacol.* **741**: 281–289.
- Sarangi S, Pandey A, Papa AL, Sengupta P, Kopparam J, Dadwal U, Basu S, Sengupta S. 2013. P2Y12 receptor inhibition augments cytotoxic effects of cisplatin in breast cancer. *Med. Oncol.* **30**: 567.
- Schellenberg B, Wang P, Keeble JA, Rodriguez-Enriquez R, Walker S, Owens TW, Foster F, Taniaris-Hughes J, Brennan K, Streuli CH, Gilmore AP. 2013. Bax exists in a dynamic equilibrium between the cytosol and mitochondria to control apoptotic priming. *Mol. Cell* **49**: 959–971.
- Shaili E. 2014. Platinum anticancer drugs and photochemotherapeutic agents: recent advances and future developments. *Sci. Prog.* **97**: 20–40.
- Song G, Chen GG, Hu T, Lai PB. 2010. Bid stands at the crossroad of stress-response pathways. *Curr. Cancer Drug Targets* **10**: 584–592.
- Szegezdi E, MacDonald DC, Ni Chonghaile T, Gupta S, Samali A. 2009. Bcl-2 family on guard at the ER. *Am. J. Cell Physiol.* **296**: C941–C953.
- Takeuchi O, Akira S. 2010. Pattern recognition receptors and inflammation. *Cell* **140**: 805–820.
- Truong Do M, Gyun Kim H, Ho Choi J, Gwang Jeong H. 2014. Metformin induces microRNA-34a to downregulate the Sirt1/Pgc-1 $\alpha$ /Nrf2 pathway, leading to increased susceptibility of wild-type p53 cancer cells to oxidative stress and therapeutic agents. *Free Radic. Biol. Med.* **74**: 21–34.
- Victorino VJ, Pizzatti L, Michelletti P, Panis C. 2014. Oxidative stress, redox signaling and cancer chemoresistance: Putting together the pieces of the puzzle. *Curr. Med. Chem.* **21**(28): 3211–3226.
- Wiese AG, Pacifici RE, Davies KJA. 1995. Transient adaptation of oxidative stress in mammalian cells. *Arch. Biochem. Biophys.* **318**: 231–240.
- Worden FP, Moon J, Samlowski W, Clark JI, Dakhil SR, Williamson S, Urba SG, Ensley J, Hussain MH. 2006. A phase II evaluation of a 3-hour infusion of paclitaxel, cisplatin, and 5-fluorouracil in patients with advanced or recurrent squamous cell carcinoma of the head and neck: Southwest Oncology Group study 0007. *Cancer* **107**: 319–327.
- Xuan H, Li Z, Yan H, Sang Q, Wang K, He Q, Wang Y, Hu F. 2014. Antitumor activity of Chinese propolis in human breast cancer MCF-7 and MDA-MB-231 Cells. *Evid. Based Complement. Alternat. Med.* **2014**: 280120.
- Yang E, Korsmeyer SJ. 1996. Molecular thanatopsis: a discourse on the BCL2 family and cell death. *Blood* **88**: 386–401.

## Supporting information

Additional supporting information may be found in the online version of this article at the publisher's web-site.